

We are IntechOpen, the world's leading publisher of Open Access books Built by scientists, for scientists

6,900

Open access books available

185,000

International authors and editors

200M

Downloads

Our authors are among the

154

Countries delivered to

TOP 1%

most cited scientists

12.2%

Contributors from top 500 universities



WEB OF SCIENCE™

Selection of our books indexed in the Book Citation Index
in Web of Science™ Core Collection (BKCI)

Interested in publishing with us?
Contact book.department@intechopen.com

Numbers displayed above are based on latest data collected.
For more information visit www.intechopen.com



Radon Calibration System

Ayman M. Abdalla, Ahmed M. Ismail and
Tayseer I. Al-Naggar

Additional information is available at the end of the chapter

<http://dx.doi.org/10.5772/intechopen.69900>

Abstract

In this chapter, an irradiation radon system was explained in detail. This system is based on soil gas as a natural radon source. The radon system was used to determine both the calibration factor of the radon detector and the equilibrium factor between radon and its short-lived daughters. Also, the calibration factor has been calculated theoretically and experimentally. The effect of humidity upon the calibration factor has been investigated. The diffusion of radon through polyethylene membrane has been determined using new nuclear method. This method depends upon the physical decay of radon.

Keywords: radon detection techniques, calibration system

1. Introduction

Radon $^{222}_{86}\text{Rn}$ is a naturally occurring noble element, radioactive gas, colorless, odorless, soluble in water, and chemically inert radioactive element. The importance of radon gas comes from its benefits in the field of uranium exploration, testing the permeability of gases in polymer membranes and its harmful effects on health. In this chapter, we will try to discuss briefly radon sources, methods of radon detection, and radon calibration system including the methods of determining the calibration factor for radon measurement experimentally and theoretically. The measurement of radon permeability through polyethylene membranes using scintillation detectors will also be discussed as a useful application in the field of radon measurement.

2. Radon sources

The three naturally produced isotopes, radon (^{222}Rn from ^{238}U series), thoron or thorium emanation (^{220}Rn from ^{232}Th series), and actinon or actinium emanation (^{219}Rn from ^{235}U series), are all disintegrated by producing alpha particles (**Table 1**) [1].

Isotope	Common name	Half life	Decay series
²²² Rn	Radon	3.8 days	²³⁸ U
²²⁰ Rn	Thoron	54.5 s	²³² Th
²¹⁹ Rn	Actinon	3.92 s	²³⁵ U

Table 1. Radon isotopes.

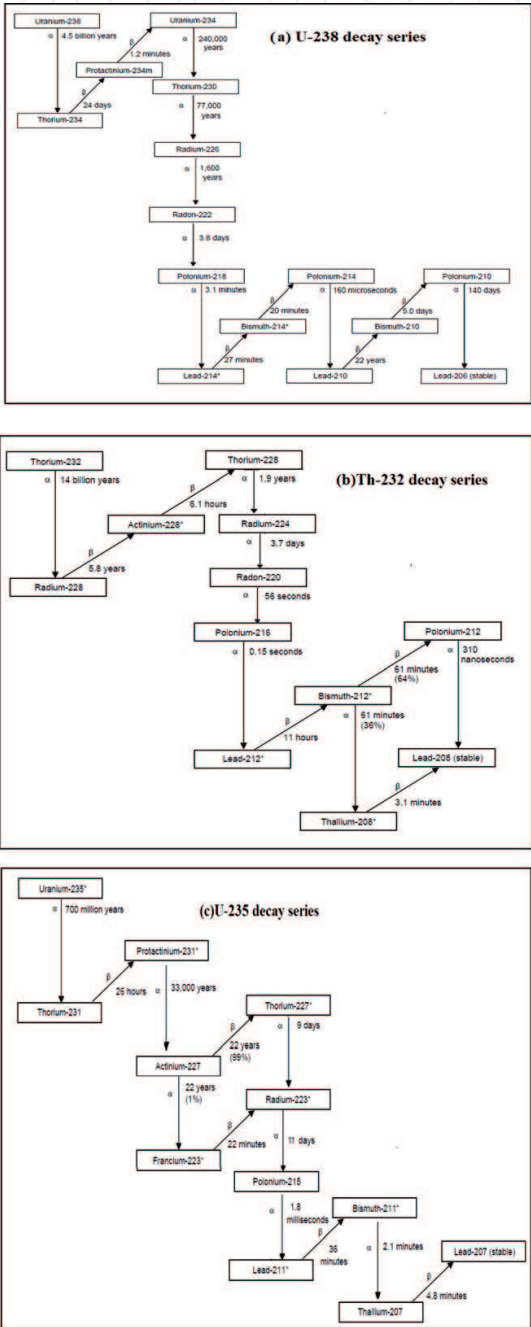


Figure 1. Three natural decay series [3].

Radon produced from uranium decay series. It is known that all types of rocks contain various amounts of uranium especially mountainous areas [2]. Radium is produced through radioactive decay of the three natural chains (^{238}U , ^{235}U , or ^{232}Th), and radon isotopes are produced as a result of radium decay (**Figure 1a–c**).

3. Radon measurement techniques

Measurement, and detection of radon can be done by two ways directly by itself (^{222}Rn only) or indirectly by its progenies. Detection and measurement of radon can be accomplished with α , β , or γ radiation detection. One of the following techniques can be used for detection: nuclear emulsion, adsorption, solid scintillation, gamma spectroscopy, beta monitoring, solid-state nuclear track detector (SSNTD), electrometer or electroscopes, ionization chambers, surface barrier detectors, thermoluminescent phosphors, electret, and collection. Radon-222 can be measured by passive method when radon enters the detection volume by just diffusion, or active, which contains the pushing of gas into or through a detecting instrument.

3.1. Passive devices

The detection sensor is commonly put inside a vessel that has an opening to allow radon to enter it. The vessel is intended to keep the detector and to make an area about the detector for a sensitive size large enough so as to have as many α -particles created and detected in as small time as possible, and in the case of direct measurement of the radiation, an inverted plastic or paper cup in various versions [4] or more advanced container can be also used.

3.1.1. Solid-state nuclear track detector

An alpha particle is detected in a SSNTD by a particular path or “trail” of damage, which after chemical etching produces a narrow channel, and it is seen under the microscope. SSNTDs such as CR-39, cellulose esters, and polycarbonates like bis-phenol-A polycarbonate are sensitive to α -particles within the energy range of the particles produced by radon. The SSNTDs are more sensitive to charged particles, on the other side, SSNTDs are more insensitive to β and γ rays, so beta and gamma rays do not serve an etchable discrete trails or tracks. However, preirradiation with nontrack forming radiation has also been found to increase sensitivity and etching speed [5]. There are various types of polymer detectors such as polyallyldiglycol carbonate (CR-39), cellulose nitrate (LR-115), and polycarbonate (Lexan, Makrofol) [6, 7]. SSNTDs do not need an energy source to work, so their detecting property is an essential quality of the substance they are made of. They are consequently very well suitable for long-term measurements in the field, so they have received special awareness. The methods in which SSNTDs are used for the detection of radon and/or radon progenies which, change generally in the geometry of the arrangement, commonly the use or not of diffusion membranes; and the use (or not) of filters to keep progenies out of equipment [8]. In other states, the detector is located vertically [9]. Some procedures have two measuring chambers, detached or not by a filter and/or a membrane. In some cases, SSNTDs are used in conjunction with another

type of detector. For instant SSNTDs can be combined with electrets. In this way, a prompt response can be obtained together with an energy differentiation [10].

3.1.2. Alpha card

The alpha card technique is a passive radon detecting process which supplies a means for accurate measurements of radon in soil gas, with dimensions $4.5\text{ cm} \times 5\text{ cm}$, and diameter hole (205 cm) punctured in the interior of it. The hole is completely closed with a slight film. Silicon detectors are used to measure the activity of alpha card in terms of alpha particles. The evaluation of reading method consists of two silicon detectors facing one another, between which the card is placed. A slightly good counting efficiency is attained because the assembling membrane is very thin, which alpha particles issuing from both sides of the card impinge upon either one of the silicon detector. The alpha card reader is a small, movable with operated battery supply that can be used in the field, and the common reading time is about 5 min [11].

3.1.3. Electrets detector

The electret radon monitor is a new technique which is used in the field to measure the radon concentration [12]. Electret is a portion of dielectric material that displays a nearly lasting electrical charge if not otherwise worried. This charge yields a robust electrostatic field which is able to assemble ions of the contrary sign and the overall charge of the electret reductions. This property can be used to make gamma radiation detectors away from the electrets [13]. The concept is not enough till the modern progress of high dielectric fluorocarbon polymers, which have turned electrets to be trustworthy, electronic constituents until under high temperature and moisture provisions. The main components of a radon monitor electret are steel canister and the electret dosimeter which is stable on the internal upper. At the lower of such canister little inlet allows the radon gas to reach the assembly during a filter. The ions are produced from radon which produces ionizing particles inside the volume of the device. The ions are assembled, and the full charge of the electrets changes; after some time has passed, the surface potential of the electret is measured by the shutter method [14–16] using a battery-operated, lightweight piece of equipment.

Detector sensibility and dynamic field are based on the size of the chamber of the equipment and of the thickness of the sensitive substance. As for solid-state nuclear track detector (SSNTD), varied geometrical preparations have been designed. For case, the measurement can be actuated time wise by having a dynamic segment translating, the electret in the lodging [17]. Detection of radon alone is achieved by using a 4π -geometry chamber, on the wall of which another electret is placed for daughter detection [18]. In some other instances, a positively charged electrode can be coated with a SSNTD or with a TL phosphor for completeness of detection and measurement.

3.1.4. The mechanism of chemical absorption

In chemical absorption mechanism, the radon dimension structure constructed on the chemical absorption of the gas on an adsorption medium such as charcoal, and then on the determination the activity of the restricted daughters ^{214}Pb and ^{214}Bi . When the adsorbing medium is

actuated charcoal, the system is well with name ROAC (radon on activated charcoal) technique. The instrument for the chemical absorption of the radon is a plastic even when the can is placed inside the place contain radon gas, with its lid open, and left in place for a few days, typically from 4 to 12 days. The container is then returned, and the cover locked. It is then transported to the laboratory where gamma activity is specified using NaI scintillation counter. Radon activity can be achieved at the check point from the decay activity curves, after adequate calibration.

By this method, thoron assay is disappeared, and the count rate must be for radon only [19] found it is possible to determine the ratio between thoron and radon emanation from a soil. Another way of determining the amount of radon is to desorb it into scintillation liquid and to count the alpha, and beta activity by liquid scintillation [20].

3.1.5. Thermoluminescent detectors

When an ionizing particle moves through a crystal, some electrons liberate from its main sites into the conduction band. The electrons are then restricted into faults of the crystal and kept there in a very constant site, and the electron can leak if the crystal is heated. As a result of recombination with the holes in the valence band, or with recombination centers, by process of radioactive, light is liberated [21, 22]. Thermoluminescent dosimeters (TLDs) are built on this attitude, in the state of radon discovering, which depends upon the alpha activity of the radon progenies. Radon can inside a detection volume include the TLD.

At a small distance, the steel plate is placed facing TLD. Radon progenies summated on the plate and eventually decay, thus creating energy storage in the TLD. After proper exposure to the radon-rich atmosphere, the TLD is recovered and “read” in a TLD apparatus. The concentration of radon is appearing on a TLD device after suitable exposure to the radon abundant air. This device is basically a little furnace, and here the heat is advanced under a nitrogen atmosphere at a very fully controlled rate. The TLD produces quantity of light that falls on the photocathode of a photomultiplier and then is transported into an electrical signal. TLD spectra are noted. Every peak relates to a particular trap, and the amplitude and/or the area below a peak is proportional to the radiation dose. In many commercially available devices, various types of detectors containing TLD sensors have been used field measurements, and in the sphere of different applications. They are using them for detecting oil gas reservoirs [23].

The advanced detection method, which really keeps an electret detector for gamma-background gauge, has three TLDS [24]. One is a preirradiated TLD which provides information on the natural fading of the signal recorded in the two others. The signal related to the radioactivity created by the radon, which has spread to the detection bulk, and the next makes a cross measurement of the γ -field. In certain cases, the housing of the TLD sensor is made such that the full detector can resist the heat at which the light is emitted from the TLD when reading it [25].

3.1.6. Solid-state electronic detectors

Solid-state electronic detectors (SSEDs) are not widely used for radon detection because it needs considerable quantity of energy not simply obtainable in the field, and also it is slightly

costly and brittle. One may mention, for instance, the Alpha meter, which the active part of the equipment is a Si(Li) detector associated with a counter unit, both operated on batteries. The counting is directly displayed on the instrument [1]. A special version of the radon devices allows water level, temperature, and conductivity measurements to be made in the meantime. The detector is especially produced for indoor measurements [26]. The measuring instrument with a hemispherical bell chamber is fitted with a solid-state alpha detector built by Ref. [27]. Several active cells for counting radon daughters use by Ref. [28]. The device based on light measurement with solid-state detectors is built by Ref. [29].

3.1.7. Ion chambers and electrometers

Apparatuses depend on the measurement of ion pairs produced through the way of α -particles in the air. The measurement can be achieved by using ion chambers and electrometers. At the first status of detection part, the amount of electrical charges can record, which have been formed without laying stable voltage. Through a second state, one assembles the electrical charges that have been produced between two electrodes in an electrical field [1].

3.2. Active devices

In active apparatuses, radon gas is either pumped from the surrounding or removed by means of a gas or liquid. In addition, the lively part for measuring radon or its progenies results is an electrical or electronic device in public. By applying a fan or a pump, many of the apparatuses up could be turned into an active apparatus. The detector where radon is propelled from the ground soil is built by Ref. [30]. The gas drift pushes through the electronic meter to the external of the instrument. Radon concentration is then determined. Direct scintillation can also be used for detecting the radon level by forcing air through the detector [31]. The other type of active detection is radon sampling or extract sampling. After sampling, the water or air or the solvent that holds radon is taken to the laboratory for detection. Sampling methods are various, but they all need one to be specially wary not to pollute the sample. Sampling can be accomplished by syringes, compressor, vacuum container, water sampling, degassing on the spot, suction action of pumps, and so on.

4. Radon irradiation chamber and its applications

Radon is a worldwide problem because inhalation of radon engages more than 50% from total natural radiation dose to the world population [3]. Radon and its short-lived decay products caused lung cancer in the USA according to the Environmental Protection Agency (EPA) [32], and the short-lived decay products of radon are responsible for most of the hazard by inhalation. The main environmental source is the soil gas emanation in dwelling areas or from building materials [33]. Solid-state nuclear track detector (CR-39) is used widely to determine the concentration of radon [34]. The calibration factor converts the track density to radon concentration and can be calculated from the relation below [35, 36]:

$$K = \frac{\rho}{c_0 t_0} \quad (1)$$

where ρ : track density (track cm^{-2}), C_0 : radon concentration (Bq m^{-3}), t_0 : exposure time (day).

The annual effective dose rate (ED, mSv/y) of inhaled radon and its progeny can be estimated according to the following equation [37]:

$$\text{ED} = C_0 F T D \quad (2)$$

where F : equilibrium factor, D : dose conversion factor ($9 \text{ nSv h}^{-1}/\text{Bq m}^{-3}$), T : average indoor occupancy time per person (7000 h y^{-1}), C_0 : radon activity concentration in air (Bq m^{-3}).

The equilibrium factor is defined as the ratio of potential alpha energy concentration (PAEC) of actual air radon mixture (also radon progeny) to the PAEC in secular equilibrium with radon [38].

$$F = \frac{(\text{PAEC})_{\text{air radon mixture}}}{(\text{PAEC})_{\text{equilibrium}}} \quad (3)$$

There are two methods to estimate the equilibrium factor: one method uses silicon surface barrier detector by the following equation [39]:

$$F = \gamma_1 \frac{C_1}{C_0} + \gamma_2 \frac{C_2}{C_0} + \gamma_3 \frac{C_3}{C_0} + \gamma_4 \frac{C_4}{C_0} \quad (4)$$

where C_0 , C_1 , C_2 , C_3 , and C_4 are the activity concentrations of ^{222}Rn and its short-lived progenies ^{218}Po , ^{214}Po , ^{214}Bi , and ^{214}Po , respectively, and the coefficients γ_i are constant.

In another method, a solid-state nuclear track detector was used to evaluate the equilibrium factor by the following equations [40, 41]:

$$D = K(C_0 + C_1 + C_4) \quad (5)$$

$$D_0 = K(C_0) \quad (6)$$

Eqs. (5) and (6) are related the respective track densities D and D_0 to the activity concentrations of radon and its progeny in air, and K is the detector sensitivity coefficient.

The equilibrium factor can be calculated by using the LR-115 detector, using the following equation [40]:

$$F = 0.47 \left(\frac{D}{D_0} \right) - 0.47 \quad (7)$$

For the CR-39 track detector, the equilibrium factor can be determined by the following equation [42]:

$$F = ae^{\left[-b\left(\frac{D_0}{D}\right)\right]} \quad (8)$$

where the values of two constants a , b are 14.958 and 7.436, respectively.

4.1. Preparing a radon source

The amount of ^{226}Ra and ^{222}Rn produced in rocks and soils depends on its ^{238}U contents, and many studies considered a variable alternative of using soil gas as a radon source in the experimental studies [43]. High-performance gamma-ray spectrometry (DSPECjr2.0) was used to measure the activity of ^{226}Ra in the soil sample; 0.424 kg of soil sample was fitted into a Marinelli beaker of 250 cm^3 volume. The gamma detector has resolution 2.2 KeV and relative efficiency 55% at 1.33 MeV of ^{60}Co . The recommended operating bias negative 4500 V. ^{176}Lu testing adapter and ^{137}Cs were used for energy calibration.

The specific activity of radium was measured using the following equations [44, 45]:

$$A_s = \frac{N}{(E \times P_r \times M)} \quad (9)$$

where N : counting rate for a specific gamma line, E : detector efficiency, P_r : absolute transition probability of γ -decay, M : mass of the sample (kg). In this work, the average specific activity of ^{226}Ra in the soil sample was $182 \pm 13\text{ Bq kg}^{-1}$. Metallic cylindrical drum with 24.7 l contains different amount of soil from the environment, used as radon source, and was covered with a polyethylene membrane to make the thoron (^{220}Rn) gas outside the system. The concentration of radon was changed using different amounts of soil.

4.2. Radon irradiation system

A radon system consists of the following parts as shown in **Figure 2**:

- 1—plastic vessel, 2—monitor, 3—lucas cell, 3, 4—printer, 5—radon source, 6, 7—PID controlled furnaces, 8, 9, 13, 14—inlet and outlet tubes, 10—internal pump, 11, 12—valves, 15—desiccation column, 16, 17—pored filter of polyethylene, 18, 19—circular port, 20—inactive dosimeter, 21—flowmeter, 22—computer interface.
2. The lucas cell 300A offers a proper tool for detection of radon. The cell was ready at a great-efficiency scintillator of silver-activated zinc sulfide. Lucas cell volume is nearly 272 ml, sensitivity of 0.037 cpm/Bq/m^3 , MDA of 27.4 Bq m^{-3} , and $E\alpha$ of 4.5–9 MeV [46]. The pump of AB-5's can be used to withdrawal air into the Lucas cell by the porous polyethylene filter, and any radon gas in the spread air decays into its daughter products, some of which are liberating α -particles. Alpha particles were hit the scintillator, which lines the inner of the Lucas cell, and create light pulses which they are amplified and 30 counted in the AB-5. A microprocessor in the AB-5 is used to convert the signal into an average count value per minute (C), and the net count value (N) is obtained by correcting the background [47].

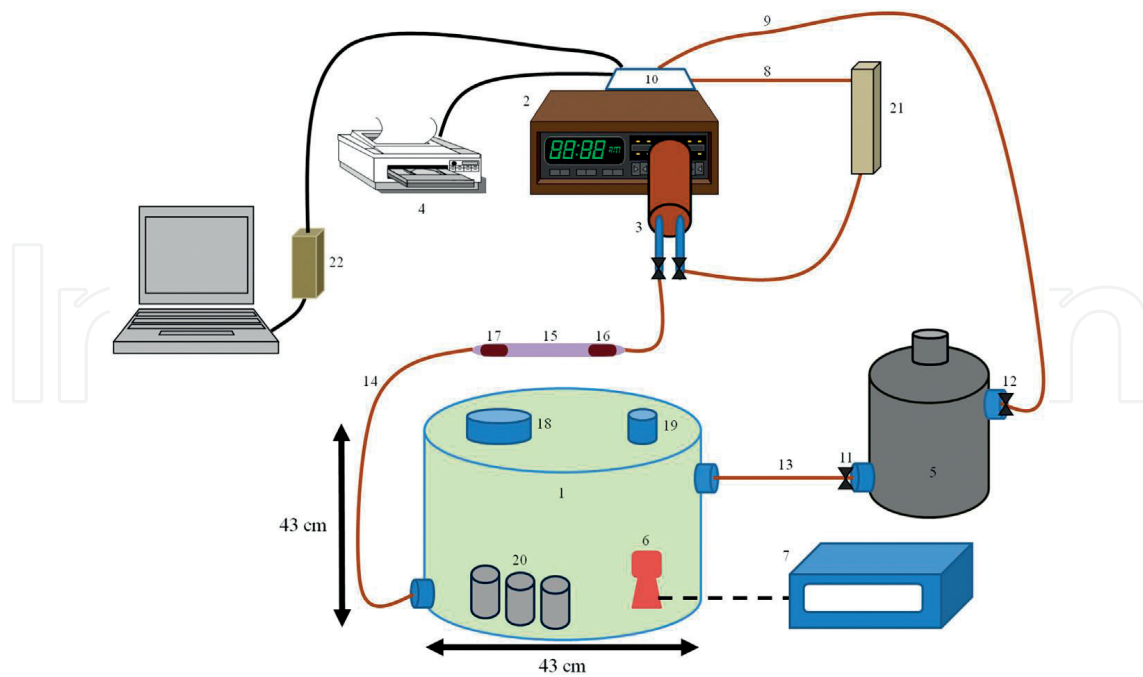


Figure 2. Radon irradiation system.

Radon gas concentration was determined by the general formula used by the AB-5 in the radon mode:

$$C_0 = \frac{NCPM}{S} \quad (10)$$

where, C_0 : radon gas concentration (Bq m^{-3}), $NCPM$: the net count per minute, S : the counting sensitivity value (cpm/Bq/m^3).

An electronic thermometer with a liquid crystal display was used to measure the temperature inside the chamber.

4.3. Calibration factor assessment

The calibration factor of the CR-39 detector can be assessed by three cups that were used with CR-39 sheets, which had an area of $1.0 \text{ cm} \times 1.0 \text{ cm}$ and a thickness of $250 \text{ }\mu\text{m}$. The plastic cups 8 cm in height and 7 cm in diameter were used in this work, and then, the detectors were etched in 6.25 N NaOH solutions at 65°C for 6 h. The etched CR-39 samples were washed in running water and dried in air. The tracks were analyzed using an optical microscope at $500\times$, and also the background tracks were registered.

4.4. Comparative studies with the track detector

Films from LR-115 have $12 \text{ }\mu\text{m}$ thickness, which were mounted on a $100\text{-}\mu\text{m}$ transparent polyester foil, were used for two different setups was used in this work. The filtered setup is the first one, where a piece of LR-115 was stable at the end of a plastic cup. Two cups were

placed in the radon irradiation system for 1 week. The exposed LR-115 sheets were etched in 2.5 N NaOH solutions at 60°C for 100 min [48]. The track density in each sheet was calculated to obtain D and D_0 for the open and closed plastic cups, respectively. The identical procedure was repeated using the CR-39 track detector that was etched at the optimum etching condition [49]. **Figure 3a** and **b** show a typical optical image of alpha particle tracks in the LR-115 and CR-39 detectors. The equilibrium factor was measured using Eqs. (7) and (8) for the LR-115 and CR-39 detectors, respectively.

Figure 4 shows the rate of track density as a function of the radon activity concentration for the diffused CR-39 track detector. From the slope of the line, it is found that the calibration factor is 0.165 track cm²/Bq m³ d with uncertainty approximately 20%. The obtained experimental value is considerably consistent with the reported experimental values in Farid (0.199 track cm²/Bq m³ d) [50] and Mansy et al. (0.177 track cm²/Bq m³ d) [51].

Table 2 demonstrates the equilibrium factor between radon and its progeny, which was determined using three different methods: solid-state nuclear track technique, surface barrier method, and our new radon chamber. From **Table 2**, the results obtained using our new radon chambers are considerably consistent with the results of the surface barrier detector method [7]. We can obtain a stable equilibrium factor between radon and its daughters in a closed environment of a radon system which emulates a closed environment of a room.

As shown in **Figure 5a**, the equilibrium factor tends to decrease as the temperature increases (temperature range of 20–50°C for 24 h) and this is due to the temperature impact on the equilibrium factor by two chief causes: (1) the temperature reduces the equilibrium factor by effects on the radon emanation rate and (2) the temperature rises the equilibrium factor by affecting the number of radon daughters in the air [52, 53]. Also **Figure 5b** shows that the equilibrium factor at 20°C is equivalent to 2.2 times the coefficient of equilibrium at 50°C and 1.5 times the coefficient of equilibrium at 32°C. Also, the influence of the flow rate through irradiation on the equilibrium factor between radon and its daughters was obvious. The

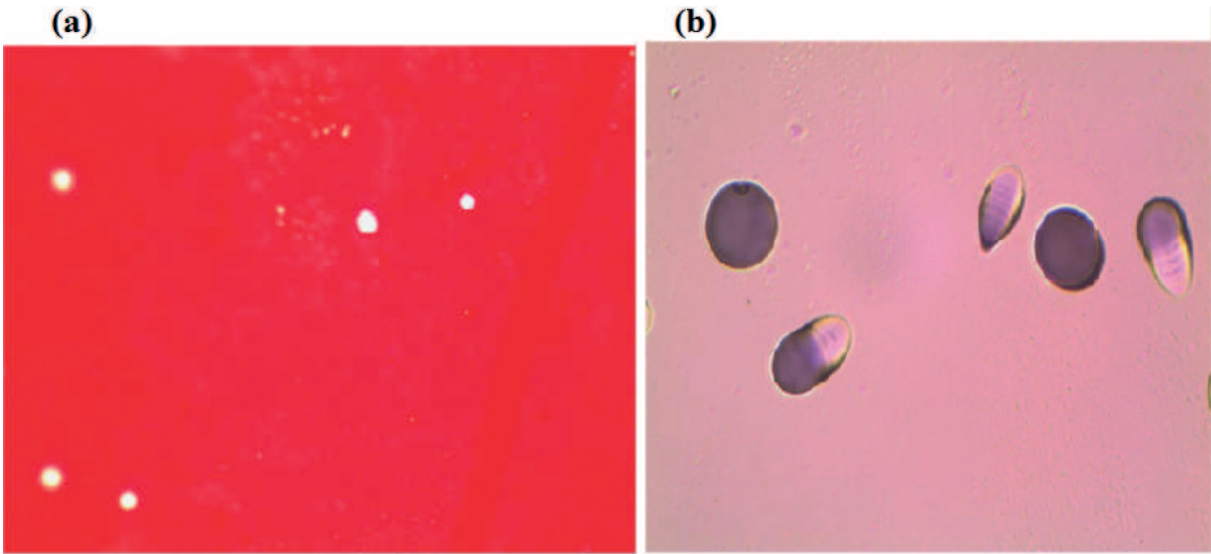


Figure 3. Track optical image of alpha particles for (a) LR-115 detector and (b) CR-39 detector.

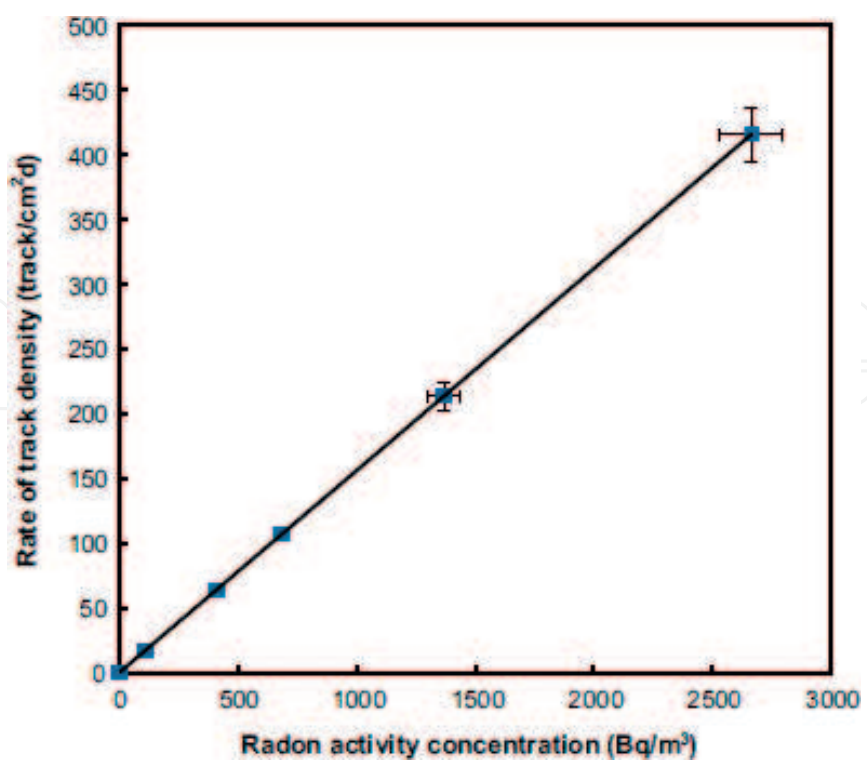


Figure 4. Rate of track density as a function of radon activity concentration.

Method	Our new radon system	SSNTD	Surface barrier detector method
Equilibrium factor	0.21	0.17 (LR-115) 0.20 (CR-39)	0.19 [5]

Table 2. Equilibriums factor obtained using three different methods.

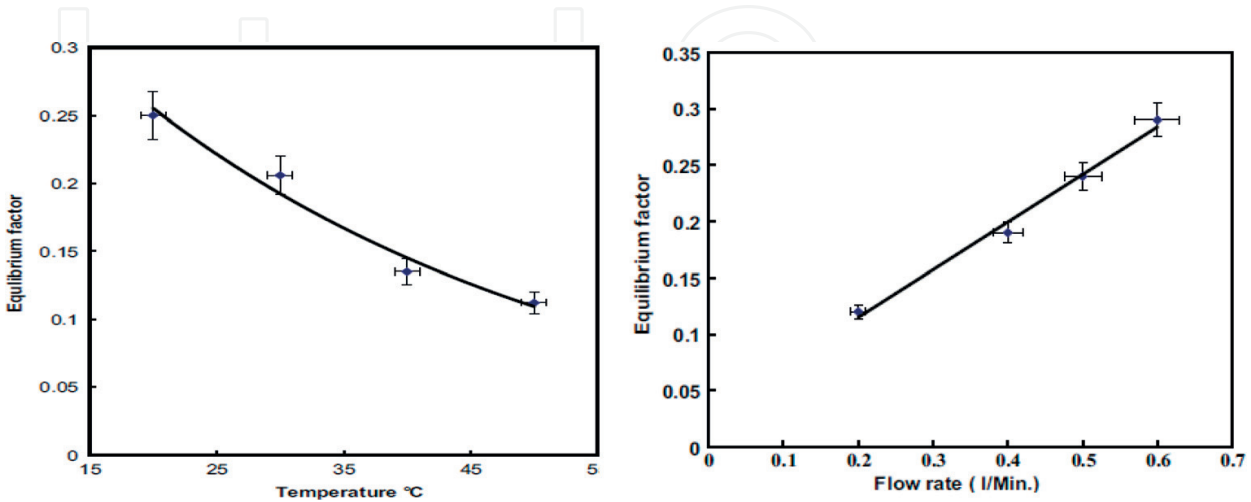


Figure 5. Equilibrium factor as a function of (a) temperature and (b) flow rate of air in the lucas cell.

system was utilized in the flow rate of 0.2–0.6 l/min for 24 h at stable heat. **Figure 5b** presents the equilibrium factor for radon, and its daughters are influenced by the variation in flow rate of radon-bearing air. The equilibrium factor rises with rising flow rate. The value of equilibrium gives 0.25 at the optimum flow rate of 0.5 l/min. These consequences indicate that the measurement of an apparent equilibrium factor as a function of the temperature and flow rate is important for determining the annual effective dose rate.

5. Radon permeability measurement through polyethylene membrane using scintillation detector

Activated charcoal technique was used to study the permeability of ^{222}Rn through polyethylene membranes. The permeability constant of ^{222}Rn through low-density polyethylene, linear low-density polyethylene, and high-density polyethylene samples has been measured, and the diffusion coefficient of radon in charcoal as well as solubility of radon in polyethylene membrane has been taken into consideration. The two gases ^{222}Rn (^{238}U -series) and ^{220}Rn (^{232}Th -series) have differences in their radioactive half-lives 3.82 days and 56 s, respectively, which provide suitable properties for their separation using proper membranes. The difference in the decay rates leads to difference in the mean diffusion distances [54, 55].

The permeability (K) of a polymer to a gas can be defined by

$$K = SD \quad (11)$$

where S : the solubility, D : the diffusion coefficient of the gas in the polymer.

The significant factor which determines the appropriateness of a membrane for separation radon isotopes is its permeability constant. Ramachandran et al. [56] suggested a method to determine the permeability constant that depends on SSNTD technique, as shown in **Figure 6**, and it is expressed by the following relation:

$$R = \frac{n_2}{n_1} = \frac{KA(V_1 + V_2)}{KA(V_1 + V_2) + V_1V_2\lambda\delta} \quad (12)$$

where R : ratio between the concentrations of gaseous in volume V_2 with a membrane and the concentration without any membrane in V_1 , K : the permeability constant ($\text{cm}^2 \text{s}^{-1}$), d : the thickness of the membrane (in cm), A : the surface area of the membrane (cm^2), and λ : the decay constant (s^{-1}).

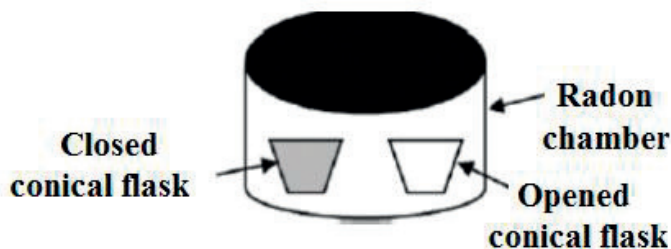


Figure 6. Schematic diagram shows solid-state nuclear track technique.

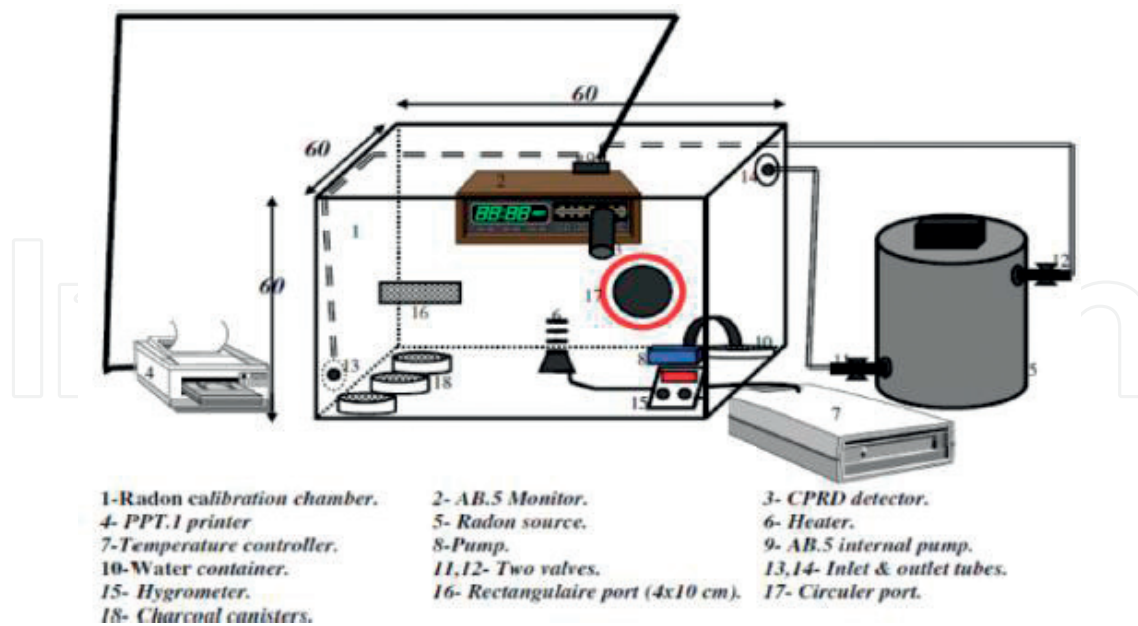


Figure 7. A schematic for radon calibration chamber.

The process used is based on exposing activated charcoal canister to radon concentration inside radon chamber [57], as illustrated in **Figure 7**.

The radon activity adsorbed by a diffusion barrier charcoal canister (DBCC) is described by the following relations given by Refs. [58–60]:

$$Q_i = \beta m C_i = V C_i \quad (13)$$

$$\frac{dC_i}{dt} = -\left(\frac{KA}{\delta V} + \lambda\right) C_i + \frac{KA}{\delta V} C_0 \quad (14)$$

$$\tau = \left(\frac{KA}{\delta V} + \lambda\right) \text{ if } P = \frac{KA}{\delta} \text{ and } \psi = \frac{1}{\tau}, \text{ Then } \psi = \frac{P}{V} + \lambda \quad (15)$$

where Q_i : the activity of radon that passes through the membrane and adsorbed by DBCC (Bq), V : equivalent to a volume of air available to the activated charcoal (cm^3), b : the adsorption coefficient of radon by activated charcoal (Bq g^{-1} per Bq cm^3), m : the mass of activated charcoal in the canister (g), C_i : the radon concentration within the canister (Bq m^{-3}), C_0 : is the radon concentration in the environment air (Bq m^{-3}), λ : the decay constant of radon (s^{-1}), K : the radon permeability ($\text{cm}^2 \text{s}^{-1}$), A : cross section of the diffusion barrier (cm^2), D : thickness of the diffusion barrier (cm), and S : is the integration time constant of radon in the DBCC (s).

For $C_i = C_{i0}$, $C_0 = 0$ at $t = 0$, the solution of the Eq. (14) is

$$C_i = C_{i0} \exp\left(-\frac{t}{\tau}\right) \quad (16)$$

The radon permeability for radon in the tested membrane can be easily evaluated by using the following equation:

$$K = \frac{VL}{A}(\psi - \lambda) \tag{17}$$

Permeability of radon was measured at room temperature and a comparative moisture of 20% at exposure was finished. The canisters were closed and left for 3 h. Gamma spectroscopy 3'' × 3'' NaI (TI) was used to determine the gamma spectrum from each canister, as illustrated in **Figure 8**. The range of energy for gamma lines between 295 and 609 keV was achieved, and the activity of radon in the canister was determined.

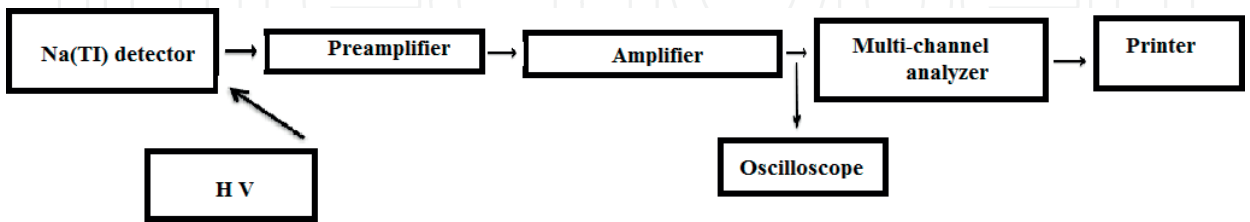


Figure 8. Schematic of the scintillation spectrometer.

Figure 9 presents the difference of the relative net count per minute as a function of time for different samples.

For SSND, pieces of CR-39 track detectors of 250 mm (TASTRAK supplied by Bristol, UK) were used for two diverse setups. In the first setup (named: filtered setup), a piece of CR-39 was stabled in the end of conical flask (250 ml), and then, the conical flask was closed with a

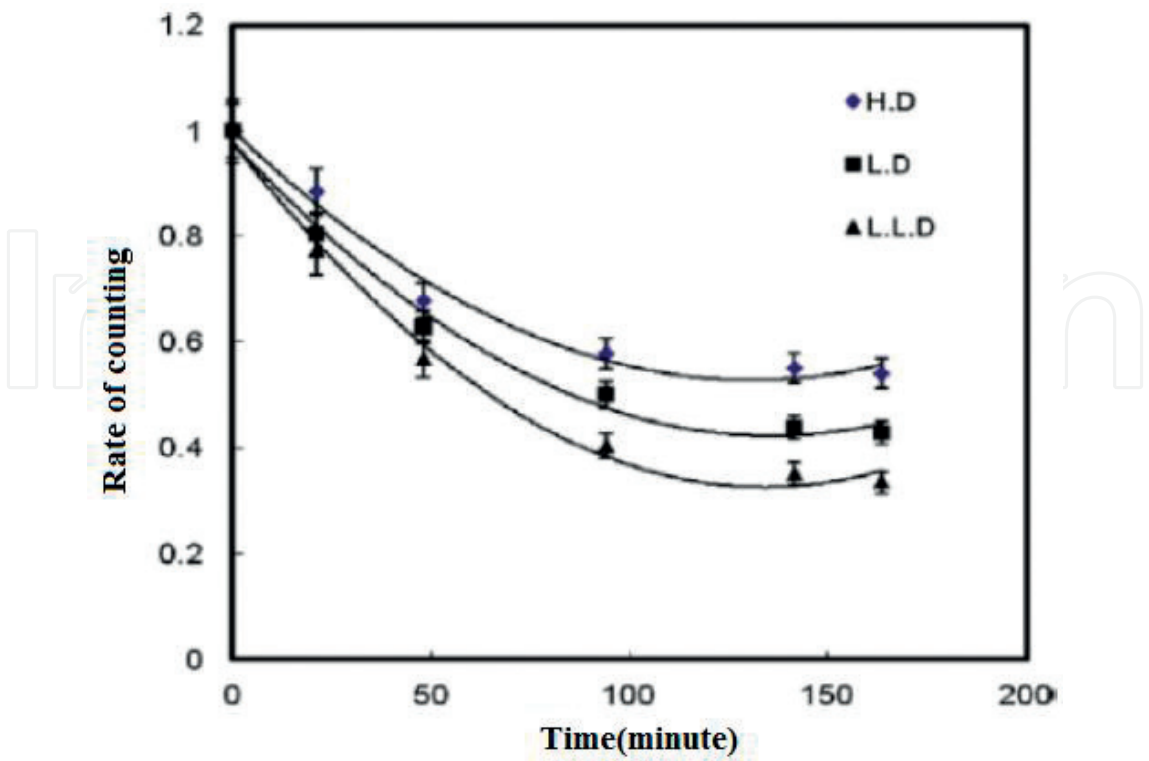


Figure 9. Rate of counting as a function of time for different polyethylene membranes.

polyethylene membrane which acts as a filter. Secondly, named bare (opened) setup, in which a piece of CR-39 was stabled at the end of opened conical flask. Filtered and open conical flasks were put in radon chamber for a term of 1 month. A diagram setup of SSNTD technique is represented in **Figure 7**. After that the CR-39 sheets have been etched in 6.25 normal NaOH solutions at 70°C .ffor 6 h. The etched samples were washed in running water and dried in air. The track density in each sheet is calculated to be n_1 and n_2 in the case of open and closed conical flasks, respectively. The radon permeability can be measured using Eq. (11).

Sample	Thickness (cm)	Track technique	Arafa method (2002)	Proposed method
LLD ^b	0.00250	1.27E−07	0.49E−07	1.5E−07
LD ^a	0.00245	1.2E−07	0.57E−07	0.9E−07
HD ^c	0.00295	1.1E−07	0.46E−07	0.46E−07

^aLD: Low-density polyethylene
^bLLD: Linear low-density polyethylene
^cHD: High density polyethylene

Table 3. Radon permeability (cm²/s) of polyethylene membrane using three different methods.

Table 3 shows the radon permeability (cm²/s) of polyethylene membrane using three different methods for high-density polyethylene samples, and the permeability of radon is stabled fined by our offered method as the same value measured by Arafa system [61] for great density polyethylene samples. For low-density polyethylene sample, there is substantial covenant between the value of radon permeability constant determined by our offered method and that of SSNT technique.

6. Theoretical calculation of the calibration factor

The calibration factor of radon dosimeter (CR-39 track detector) for radon and its daughters has been determined theoretically. Calibration factor (K) is the quantity, which is used for converting the observed track density rates to activity concentrations of the species of interest.

If ρ is the track densities observed on a SSNTD due to exposure in a given mode to a concentration C for a time t , then:

$$\rho = K C t \tag{18}$$

The signal measured by etched track dosimeters is the integrated track density (tracks cm^{−2}). If the track density is uniform over the detector surface, the signal is defined by: [62]

$$\rho = \frac{K}{\tau_r} \int_0^{t_e} C(t) dt \tag{19}$$

where τ_r is the radon decay time (5.5 days), $C(t)$ is the radon concentration in the air around the detector (atom m^{−3}) at time t , and t_e is the exposure time, K denotes the dosimeter response (calibration coefficient) and is defined by:

$$K = \frac{\tau_r}{C(t)} \frac{d\rho}{dt} = \frac{1}{A_0(t)} \frac{d\rho}{dt} \quad (20)$$

where $A_0(t)$ is the activity concentration of radon in air (Bq m^{-3}) at time t and $d\rho/dt$ is the track density production rate ($\text{tracks cm}^{-2} \text{d}^{-1}$).

For a diffusion chamber-type dosimeter with a long exposure time ($t_e \gg .3 \text{ h}$), the response can be calculated by: [36]

$$K = \frac{\rho}{\bar{A}_0 t_e} \quad (21)$$

where \bar{A}_0 denotes the average radon activity concentration and t_e is the exposure time. In general, the total track density $\rho(r)$ at the point of observation in the detector, defined by r , is the result of an integration of all α -emissions which can produce observable tracks. It can be written as:

$$\rho(\vec{r}) = \sum_i \rho_i^v(\vec{r}) + \sum_i \rho_i^p(\vec{r}) \quad (22)$$

where $\sum_i \rho_i^v(\vec{r})$: track density due to radon, Po : isotopes existing in the air, and $\rho_i^p(\vec{r})$: track density due to radon decay progenies.

Ilic reported that for every α -produced nuclide existing the air is calculated by [63]:

$$\rho_i^v(\vec{r}) = \int_0^{t_e} dt \int_{V_1} \frac{A_i(\vec{r}', t) \cos \theta}{4\pi |\vec{r} - \vec{r}'|^2} dV \quad (23)$$

where $A_i(\vec{r}, t)$: activity concentration of i th nuclide for time t and at a point r , θ : angle between the particle's trajectory and the normal to the detector surface, $|\vec{r} - \vec{r}'|$: distance between the detector surface and the source volume dV , and V_i : the sensitive to volume for i th nuclide.

The stable rate of etching is calculated by the critical angle of etching. $\theta_{c,i}$ in this event can be found as:

$$\rho_i^v = 0.25 A_i t_e R_i \cos^2 \theta_{c,i} \quad (24)$$

Eq. (23) gives the estimation of track density as a function of the radon activity and intrinsic detector efficiency [64]. K_0 can be calculated by the flowing relation:

$$K_0 = 0.25 R_0 \cos^2 \theta = 0.88 \text{ cm} = 3.2 \frac{\text{tracks cm}^{-2}}{\text{KBq m}^{-3} \text{ h}} \quad (25)$$

7. Future of radiation detection

In the last few years, radiation detection has emerged as an area of interest for quantum dots (QDs) application [65]. However, there have been very few published studies on the radiation detection based on colloidal QDs. The emission of QDs is size dependent, so the output wavelength can be tuned to the sensitivity of the PMTs or avalanche photodiodes (APD). However, the stopping power of most QDs is low and their scintillation luminescence is very weak [66]. The combination of high stopping power of inorganic scintillator with QDs could potentially lead to a new class of scintillator [67]. The aim of our future work is to develop the sensitivity and counting efficiency of radiation detector using nanoparticle.

Acknowledgements

This project was funded by King Abdulaziz City for Science and Technology, the kingdom of Saudi Arabia, grant number: 14-ENV1162-60. Financial support by King Abdulaziz City for Science and Technology is gratefully acknowledged.

Author details

Ayman M. Abdalla^{1,2*}, Ahmed M. Ismail³ and Tayseer I. Al-Naggar^{1,4}

*Address all correspondence to: aymanabdalla62@hotmail.com

1 Department of Physics, College of Science and Arts, Najran University, Najran, Saudi Arabia

2 Promising Centre for Sensors and Electronic Devices (PCSED), Najran University, Najran, Saudi Arabia

3 Physics Department, Faculty of Education, Ain Shams University, Roxy, Cairo, Egypt

4 Department of Physics, College of Women for Art, Science and Education, Ain Shams University, Cairo, Egypt

References

- [1] Durrani SA, Ilic R, editors. Handbook of Radon Measurements by Etched Track Detectors: Applications in Radiation Protection, Earth Science and the Environment. World Scientific Publishing; 1997. p. 387. ISBN: 9810226667
- [2] Hararah SMAI. Investigation of radon pollution in groundwater in the southern part of Gaza Strip—Palestine [MSc thesis]. Gaza, Palestine: The Islamic University; 2007
- [3] Human Health Fact Sheet. EVS, Argonne National Laboratory; August 2005. https://www.remm.nlm.gov/ANL_ContaminantFactSheets_All_070418.pdf

- [4] Fleisher RL, Mogeo-Campero A. Mapping of integrated radon emanation for detection of long-distance migration of gases within the earth: Techniques and principles. *Journal of Geophysical Research*. 1978;**83**:3539–3549
- [5] US Atomic Energy Commission. Personal dosimeter for radon and daughter products. U.S. Patent No. 749. 725. 680. 802;1968
- [6] Cassou RM, Benton EV. Properties and applications of CR-39 polymeric nuclear track detector. *Nuclear Track Detection*. 1978;**2**:173–179
- [7] Tommasino L. Radon monitoring by alpha track detection. In: Tommasino L, et al., editors. *Proceedings of the International Workshop on Radon Monitoring in Radioprotection, Environmental Radioactivity and Earth Science*; 1981; Trieste. Singapore: World Scientific; 1990. pp. 123–132
- [8] Yoder RC. Radon gas detector with sensing film. U.S. Patent No. 211, 516, 880, 624;1988
- [9] Wheeler RV. Detector for radon gas and its decay products. U.S. Patent No. 012; 266; 1987
- [10] Pretzsch G, Borner E, Lehmann R, Sarenio O. Radon diffusion chamber with passive integrating detector. German (former Democratic Republic) Patent No. 276, 690, 850, 528; 1985
- [11] Durrani SA, Ilic R, editors. *Handbook of Radon Measurements by Etched Track Detectors: Applications in Radiation Protection, Earth Science and the Environment*. World Scientific Publishing; 1997. p. 387. ISBN: 9810226667
- [12] Kotrappa P, Dempsey JC, Hickey JR, Stieff LR. An electret passive environmental ^{222}Rn monitor based on ionization measurement. *Health Physics*. 1988;**54**(1):47–56
- [13] Marvin HB. How to measure radiation with electrets. *Nucleonics*. 1955;**13**:82–87
- [14] Kotrappa P, Dua SK, Pimpale NS, Gupta PG, Nambi KSV, Bhagwat AM, Soman SD. Passive measurement of radon and thoron using TLD or SSNTD on electrets. *Health Physics*. 1982;**43**(3):399–404
- [15] Kotrappa P, Dua SK, Gupta PC, Pimpale NS, Khan AH. Measurements of potential alpha energy concentration of radon and thoron daughter using an electret dosimeter. *Radiation Protection Dosimetry*. 1984;**5**:49–51
- [16] Gupta PC, Kotrappa P, Dua SK. Electret personal dosimeter. *Radiation Protection Dosimetry*. 1985;**11**:107
- [17] Ramsey PM, Stieff LR. Programmable control exposure radon measurement system. U.S. Patent No. 920: 421; 1992
- [18] Gast H. Measuring chamber for determining alpha activity of radon gas in carrier gas especially air. German Patent No. 200: 308, 920, 109; 1992
- [19] Megumi K, Mjamuro T. Method of measuring radon and thoron exhalation from the ground. *Journal of Geophysical Research*. 1977;**77**(17):3052–3056

- [20] Perlman D. Method and apparatus for radon detection. European Patent No. 359: 770, 900, 328; 1990
- [21] Horowitz YS. TL Dosimetry. Boca Raton, FL, USA: CRC Press; 1984
- [22] McKeever S. Thermoluminescence of Solids. Cambridge: Cambridge University Press; 1985
- [23] Hochman MB, Ypma PJ. Location of oil and gas reservoirs. Australian Patent No.01: 988, 788, 000; 1988
- [24] Harley NH, Maiello ML. Passive measurement of environmental radioactivity. U.S. Patent No. 021, 450, 870, 304; 1987
- [25] Seidel JL. Thermoluminescent dosimeter for monitoring subsurface radiation. U.S. Patent No. 941, 995, 780, 913; 1982
- [26] Kotlyarov AA, Krivashcheev SV. Measuring chamber of volume activity of radon surrounding air samples. Russian Patent No. 2, 008, 694, 940, 228; 1994
- [27] Matthies D. Radon concentration measuring instrument. German Patent No.940, 908, from 93DE-307, 015, 930, 305; 1994
- [28] Thomson I. Radon detector. U.S. Patent No.4, 983, 843, 910, 108; 1991
- [29] Dwcuir J. Radon monitoring device. European Patent No. 357, 697, 900, 314; 1990
- [30] Iimasti V. Device for measuring radon gas concentration. Finnish Patent No.002, 717, 870, 618; 1987
- [31] US Secretary of Interior Monitoring radon gas in air. U.S. Patent No. 653, 314, 760, 129; 1976
- [32] Tirmarche M, Harrison JD, Laurier D, Paquet F, Blanchardon E, Marsh JW. Lung Cancer Risk from Radon and Progeny and Statement on Radon CRP Publication 115 Ann. ICRP **40**(1):2010
- [33] Environment Protection Agency of USA. A Citizen's Guide to Radon. 4th ed. 2002
- [34] Imtiaz N, Faheem M. Determination of ^{238}U contents in ore samples using CR-39-based radon dosimeter—disequilibrium case Radiation Measurements **41**(4):471-476
- [35] Matiullah J. Determination of the calibration factor for CR-39 based indoor radon detector. Journal of Radioanalytical and Nuclear Chemistry. 2013;**298**(1):369–373
- [36] Sutej T, Ilic R, Najzer M. Response of track-etch dosimeters to environmental radon. Nuclear Tracks and Radiation Measurements. 1988;**15**(45):547–550
- [37] UNSCEAR. United Nations Scientific Committee on the Effects of Atomic Radiation Sources, Effects and Risks of Ionizing Radiation. New York: United Nations; 2000
- [38] Dorsche IB, Piesch E. Radiation Protection Dosimetry. 1993;**48**(2):145

- [39] Jamil K, Rehman F-U, Ali S, Khan HA. Nuclear Instruments and Methods in Physics Research Section A. 1997;**388**:267–272
- [40] Planinic J, Rdolic V, Faj Z, Suvelajak B. Nuclear Instruments and Methods in Physics Research Section A. 1997;**396**:414–417
- [41] Yu KN, Leung SY, Nikezic D, Leung JKC. Radiation Measurements. 2008;**43**:S357–S363
- [42] Faj Z, Planinc J. Radiation Protection Dosimetry. 1991;**35**:265–268
- [43] Al-Azmi D. Radiation Measurements. 2009;**44**:306–310
- [44] Nooruddin I. Natural activities of ^{238}U , ^{232}Th and ^{40}K in building materials. Journal of Environmental Radioactivity. 1999;**43**:255–258
- [45] Wafaa A. Journal of Environmental Radioactivity. 2004;**75**:315–327
- [46] Pylon Electronics Inc. Models 110A&300A. Instruction Manual Number A900071; 2009. p. 12
- [47] Pylon Electronics Inc. Model AB-5. Instruction Manual Number A900024 Rev. 6; 2002
- [48] DeCicco F, Pugliese M, Roca V, Sabbarese C. Applied Radiation and Isotopes. 2013;**78**:18–112
- [49] Ashry AH, Abou-Leila M, Abdalla AM. Radiation Measurements. 2011;**46**:149–152
- [50] Farid SM. Journal of Environmental Radioactivity. 1997;**34**:29–36
- [51] Mansy M, Sharaf MA, Eissa HM, El-Kamees SU, Abo-Elmag M. Radiation Measurements. 2006;**41**:222
- [52] Chu T-C, Liu H-L. Applied Radiation and Isotopes. 1996;**47**:543–550
- [53] Singh K, Singh M, Singh S, Sahota HS. Radiation Measurements. 2005;**39**:213
- [54] Tanner AB. Radon migration in the ground: A Review. In: Adams JAS, Lowder WL, editors. The Natural Radiation Environment. Chicago: University of Chicago Press; 1964:161–190
- [55] Tanner AB. Radon migration in the ground: A supplementary review. In: Gesell TF, Lowder WM, editors. The Natural Radiation Environment III, Symposium Proceedings, Houston, Texas, April 1978, Vol. 1. U.S. Dep. Environ., Natl. Tech. Info. Serv., Washington, DC, Rep. CONF-780422, 1980
- [56] Ramachandran TV, Lalit BY, Mishra UC. Measurement of radon permeability through some membranes. International Journal of Radiation Applications and Instrumentation. Part D. Nuclear Tracks and Radiation Measurements. 1987;**13**(1):81–84
- [57] El-Sammane H, Arafa W, Abdalla A. Temperature and humidity consideration for calculating air born ^{222}Rn using activated charcoal canisters. Health Physics. 2002:97–105
- [58] Cohen BL, Cohen ES. Theory and practice of radon monitoring with charcoal adsorption. Health Physics. 1983;**45**:501–508

- [59] Cohen BL, Nason R. A diffusion barrier charcoal adsorption collector for measuring radon concentrations in indoor air. *Health Physics*. 1986;**50**:457–463
- [60] Montero Cabrera ME, Sujo LC, Villalba L, Peinado JS, Jiménez AC, Miranda AL, Herrera Peraza EF. Calibration of diffusion barrier charcoal detectors using a semi-empirical expression. *Applied Radiation and Isotopes*. 2003;**59**:281–287
- [61] Arafa W. Permeability of radon-222 through some materials. *Radiation Measurements*. 2002;**35**:207–211
- [62] Fleischer RL, Giard WR, Mogro-Compero A. *Health Physics*. 1980;**39**:957
- [63] Ilic R. *Environmental Radioactivity and Earth Sciences*. 1990;**133**
- [64] Fleischer RL, Mogro-Compero A. *Journal of Geophysical Research*. 1978;**83**:3539
- [65] Hossu M, Liu Z, et al. *Applied Physics Letters*. 2012;**100**(1):013109
- [66] Yao M, Zhang X, et al. *Journal of Applied Physics*. 2010;**108**(10):103104
- [67] Sahi S, Chen W. *Radiation Measurements*. 2013;**59**:139–143

